

Normal-incidence steering effect in crystal growth: Ag/Ag(100)

F. Montalenti* and A. F. Voter

Theoretical Division, Los Alamos National Laboratory, Los Alamos, New Mexico, 87545

(Received 21 March 2001; published 2 August 2001)

During crystal growth by vapor deposition, normal incident atoms are deflected toward three-dimensional surface structures. The effect becomes strong when the atoms are deposited with a low initial kinetic energy. At low T this steering effect induces an instability in the growth process, causing a perfectly flat surface to become rough after a few monolayers are deposited. Quantitative results for the initial stages of growth of Ag/Ag(100) at $T \sim 0$ K are presented.

DOI: 10.1103/PhysRevB.64.081401

PACS number(s): 81.10.Aj, 68.35.Ct

Understanding the microscopic mechanisms governing crystal growth has been one of the principal goals of surface science for decades. This is an ambitious goal from both theoretical and experimental points of view. Indeed, a direct experimental observation of all relevant diffusion mechanisms occurring while a crystal surface grows is still impossible. As a consequence, reliable theoretical models are needed in order to interpret experimental data. The extremely long time scales involved (minutes) and the overall complexity of the process cause serious problems when trying to simulate growth.

A recently reported discovery makes a theoretical understanding of crystal growth even more difficult. Van Dijken *et al.*¹ showed that if a Cu(100) crystal is grown by grazing-angle deposition, atoms are deflected toward three-dimensional (3D) structures, leading to a rougher surface. The effect is strongest for the most grazing angles. This experimental observation has an important consequence: the incident flux does not land homogeneously on the surface (as generally assumed in simple theoretical models). Further analysis of the grazing-incidence steering effect can be found in Refs. 2 and 3. Although the first experimental proof of the steering effect was given in Ref. 1, earlier simulations by Luedtke and Landman⁴ showed that, at non-normal incidence, noticeable trajectory deflections toward preexisting protrusions could give rise to rough surfaces.

The influence of steering on the morphology of a surface grown under normal-incidence conditions was taken into account in a very recent work by Raible *et al.*⁵ The authors proposed a nonlinear stochastic equation to describe amorphous thin-film growth, including a term which qualitatively mimics the steering effect. Such a term induces an instability in the growth process.

In this paper we consider a realistic surface, Ag(100), onto which we deposit an additional 5 ML of Ag using molecular dynamics (MD) at near-zero temperature. We show that the normal-incidence steering effect has dramatic consequences on the morphology of the growing crystal, even after only a few (2 or 3) ML, provided that the deposited atoms have a low initial kinetic energy (K_i). The effect is analyzed and quantified for different values of K_i .

Here we focus solely on growth at near-zero temperature. Besides being an interesting limit to explore, it is one we can simulate exactly. Assuming classical dynamics, all activated processes are suppressed. Thus the experimental time be-

tween deposition events ($\sim 10^0$ s) can be collapsed to a MD-accessible time of a few ps without corrupting the growth dynamics. At higher temperatures, thermal diffusion events must be taken into account to make proper predictions of the surface morphology. For typical experimental deposition fluxes (≤ 1 ML/s), this type of simulation is beyond the reach of MD by several orders of magnitude. Using the recently introduced temperature-accelerated dynamics (TAD) method,⁶ we are presently⁷ extending the analysis to higher temperatures at realistic fluxes.

We first describe the simulation procedure. The Ag-Ag interaction is modeled by an embedded-atom-method (EAM) potential.⁸ The surface is initially composed of 588 atoms (98 per layer). The bottom three layers are kept frozen and the upper three (eight after 5 ML are deposited) are moving. Among them, the lowest layer is held at $T \sim 1$ K using a Langevin thermostat and the entire system is quenched before each deposition. A new atom is deposited every 2 ps: a random position is chosen within the primary period of the surface slab, and the coordinate perpendicular to the surface is adjusted until the atom just “feels” the attractive interaction with the surface atoms. Using a 2.5-fs integration time step, the system is evolved using MD for the 2 ps until the next deposition. We considered ten different initial kinetic energies in the range [0.01,0.5] eV, and for each of them we grew 5 ML. In order to collect good statistics, 25 independent simulations were run for each initial kinetic energy.

For an ideal fcc (100) crystal where each atom is in a fourfold site, i.e., is supported by four atoms in the layer beneath, the surface roughness W^2 can be computed as⁹

$$W^2 = \sum_{j=0}^{\infty} (j - \Theta)^2 (\theta_j - \theta_{j+1}), \quad (1)$$

where Θ is the total coverage and θ_j is the coverage of layer j . However, overhanging sites (i.e., with fewer than four supporting atoms) may be occupied during crystal growth (see below, and in Refs. 10 and 11), so that Eq. (1) does not hold. Consequently, we use the following more general approach to compute W^2 . The height (h) of the surface at any (x, y) point is defined as the z (normal) distance above the surface at which a probe sphere of diameter d_p would just touch the nucleus of some surface atom. Using a square grid of (x, y) points, we determine the variance in h , W_s^2 . A 50×50 grid gives good convergence in this case. In this approach, the

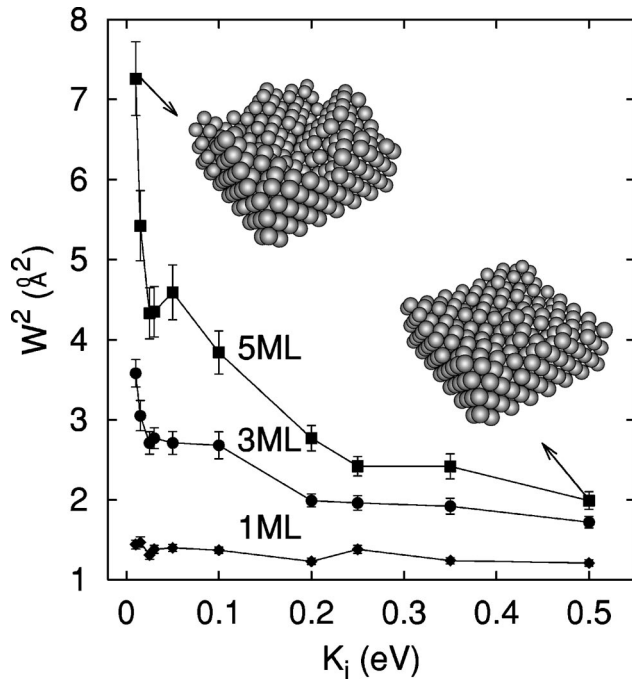


FIG. 1. Roughness (W^2) vs K_i at $T \sim 0$ K after 5 ML (upper curve), 3 ML (intermediate), and 1 ML (lower). Error bars represent a single standard deviation of the mean, computed by averaging over 25 independent simulations. Insets: typical geometry after 5 ML for $K_i = 0.01$ eV (left) and $K_i = 0.5$ eV (right).

clean surface has a nonzero variance (W_c^2), so the desired surface roughness must be computed as $W^2 = W_s^2 - W_c^2$. When $d_p = d_1$ (nearest-neighbor distance), for a surface with only fourfold sites occupied and no interlayer relaxation, this method should give the same roughness as Eq. (1). We verified this numerically. If d_p is increased, it corresponds to a lower-resolution surface probe, which may be desirable in some studies. For $d_p < d_1$, there are certain (x, y) positions where the probe can pass through the entire crystal without touching a single nucleus, giving an infinite roughness. For the present study, we increased d_p slightly to $d_p = 1.1d_1$; this improves the convergence properties by staying clear of this singularity.

In Fig. 1 the surface roughness W^2 , after 1, 3, and 5 ML, is plotted against the initial kinetic energy. Typical experimental values ($K_i \sim 0.1$ eV) are within the range we analyze. For a coverage of 1 ML, no clear effect of steering on the roughness is revealed. However, after 3 or more ML, decreasing K_i clearly increases the roughness, and the resulting surfaces are qualitatively different, as shown in the insets of Fig. 1 for a typical crystal geometry after 5 ML for $K_i = 0.01$ eV (left) and $K_i = 0.50$ eV (right). For the lower K_i , seven layers are partially occupied, and holes and 3D structures are clearly visible. In contrast, for $K_i = 0.5$ eV, the surface is relatively smooth; 6 layers are occupied, with the lowest three completely filled, and the fourth has a 98% coverage.

Why are the two surfaces so different? It should be emphasized that the observation of a roughness decreasing with K_i was already reported in the literature.¹² Nevertheless, the

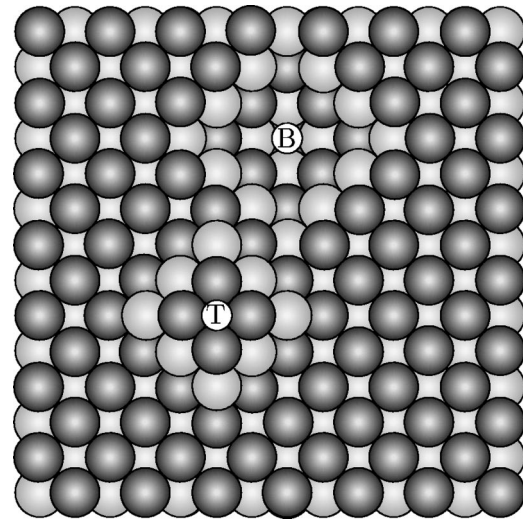


FIG. 2. Model surface, used for emphasizing the role of the steering effect. The surface contains a small pyramid and a hole. Atoms in the same layer are represented with the same gray level (as in Fig. 3). Letters T and B represent free fourfold sites on top of the pyramid and at the bottom of the hole, respectively.

effect was attributed to a *transient mobility* of the impinging atom following the first impact with the surface: for higher K_i the surface is smoother, since the atom can use its extra energy after the impact to funnel down¹³ from where it hits. Here we claim that transient mobility plays a secondary role for very small K_i , its role becoming more important only for the highest values of K_i in our range. Further, we affirm that the roughness behavior shown in Fig. 1 is mainly due to a steering effect: as soon as the impinging atom starts feeling the interaction with the outermost surface atoms, it will deviate toward them. As K_i is lowered, this lateral force acts for a longer time, giving a greater lateral displacement. As is well known, every atom strongly accelerates toward the surface during the deposition process. In our simulations, each Ag atom gains ~ 1.3 eV before impacting the surface. Because of the very low values of K_i , it would be hard to justify the behavior shown on the left side of Fig. 1 with a generic transient mobility of the atom after the impact, since the atoms land on the surface with a very similar kinetic energy. In the steering effect, on the other hand, it is the initial kinetic energy that counts, and not the kinetic energy after the impact. As a consequence, for very low K_i , even a change of a few meV can induce a noticeable change in the surface morphology. Note that the steering effect causes surface roughness in two qualitatively different ways. If the surface contains a high three-dimensional structure, impinging atoms will be deflected toward it, causing a further growth of the structure (*direct steering effect*). Further, if the surface contains a hole, impinging atoms with a low K_i are likely to be attracted to the sides of the hole, less often reaching the bottom (*inverse steering effect*). Both events obviously enhance the surface roughness.

We now show with a simple example how strong the steering effect can be at low K_i . We consider the artificially built surface displayed in Fig. 2, which contains both a truncated pyramid and a pyramidal hole. Both on top of the

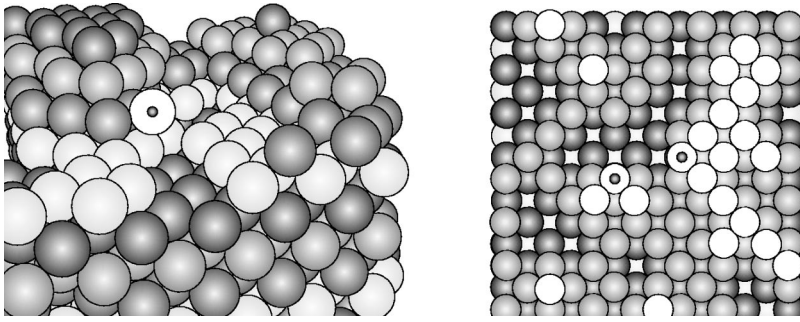


FIG. 3. Examples of two different overhanging sites. Left panel (the surface is conveniently rotated): the white circle with a black dot in the center represents an atom occupying a typical 111-like site located on the side of a 3D structure. Right panel (top view): the two white circles with a black dot in the center represent atoms occupying a threefold, i.e., a site with only three supporting atoms in the layer below.

pyramid (site T in the figure) and at the bottom of the hole (site B), there is one fourfold site that may be occupied by an impinging atom. We chose 10^4 random initial positions, and we deposited one additional atom on the surface, monitoring its final position. The simulation was performed for $K_i = 0.01, 0.1, \text{ and } 0.25$ eV. There were 407, 261, and 169 final configurations with the atom on top of the pyramid, respectively, whereas the atom landed on the site at the bottom of the hole 0, 19, and 67 times, respectively. These results clearly confirm that at low K_i , atoms tend to be steered toward protrusions and away from the bottoms of holes. For $K_i = 0.25$ eV we note that the impinging atom is helped to reach the hole by transient mobility: it bounces against the sides of the hole before reaching its bottom. As anticipated, for the highest values of K_i considered in this paper, the transient mobility cooperates in inducing a smooth surface. In this example, the surface already contained a 3D structure and a hole. Of course, in the growth simulations, we started with a flat surface. Nonetheless, after 5 ML the surfaces grown with lower K_i are very rough. Indeed, the steering effect causes a clear instability in the growth process (see Ref. 5): even starting from a perfect defect-free surface, sooner or later a small protrusion will be created on the surface. If K_i is low enough, the impinging-atom flux will start to be deflected, causing a quick enlargement of the protrusion.

We note that the embedded-atom potentials used in this simulation⁸ have a 5.54-Å cutoff distance, whereas in the real system an atom first feels the surface at a much larger distance.^{1,14} We observe a strong roughening even with the short-ranged potential, so the effect may become dramatic in real systems, particularly for $K_i \sim 0$ and thicker films. As a rough test, we extended the cutoff for incoming atoms to 20 Å by replacing the EAM Morse pair potential with a 6-12 Lennard-Jones potential matched to the basin shape of the Morse potential. We deposited 5 ML on a flat Ag(100) surface with $K_i = 0.025$ eV (an energy where steering affects the roughness strongly). The average roughness of the surface after 1 and 2 ML were the same, within a single-standard-deviation error bar, as obtained with the short cutoff. After 3 and 4 ML, a rise in the roughness was detected in the long-cutoff simulations, but still the results did not deviate by more than two standard deviations. After 5 ML, on the other hand, the surfaces generated with the long cutoff start to become clearly rougher, increasing W^2 by $\sim 30\%$. For a slightly larger K_i (0.1 eV), the longer cutoff does not change the roughness even after 5 ML. Although the trajectories are

qualitatively different, with the long-cutoff atoms starting their deflection earlier, the increased deflection is not enough to allow the newly deposited adatoms to land on a higher layer, and the roughness is thus unchanged. Of course, this is not a general argument: if a sufficiently high 3D structure is formed on the surface (as is likely to happen for a final coverage of several ML), a long-range interaction must induce a rougher surface, the effect being particularly strong for low K_i .

Another interesting feature of the surfaces grown in our simulations is the occupancy of overhanging sites and the formation of bulk vacancies. (see Ref. 10). Two typical non-fourfold sites are shown in Fig. 3. We verified that decreasing K_i , the overhanging-site population grows, ranging, at a total coverage of 5 ML, from $\sim 7.5\%$ of the deposited atoms for $K_i = 0.01$ eV to $\leq 1\%$ at $K_i = 0.5$ eV. In our opinion, both steering and transient mobility are responsible for this behavior. Indeed, overhanging sites are abundant on the sides of 3D structures, (111-like sites are found on the sides of a pyramid such as the one displayed in Fig. 2), so that atoms deflected toward the structure may occupy one such site. As shown by Sanders and DePristo,¹⁵ when the impinging atom hits a fourfold site, no transient mobility is detected. But overhanging sites are less stable than fourfold sites and they are often less symmetric (see the right panel of Fig. 3) than a fourfold site. As a consequence, an atom can escape more easily from an overhanging site, after it lands in its attraction basin. From our simulations, we verified that the probability of sticking to a nonfourfold site after being deposited over it decreases with K_i (similarly, it was found to decrease with the temperature in Ref. 16). For $K_i \geq 0.1$ eV, the fraction of deposited atoms that do not stick on an overhanging site because of this transient mobility effect becomes non-negligible. For $K_i \sim 0.5$ eV, only fourfold sites are found to be occupied, and the deposition process seems to closely follow the funneling picture of Ref. 13. Vacancy formation is strictly related to overhanging-site population. Indeed, the easiest mechanism for vacancy formation requires an empty fourfold site to be covered by four overhanging sites in the layer above.¹⁰ For $K_i \geq 0.2$ eV, the occupied sites are mainly fourfold, so that no vacancies at all were found during the 5-ML deposition. Only for $K_i \sim 0.1$ eV, on average, did one vacancy per simulation start to appear in our grown films. For $K_i = 0.01$ eV, ~ 2 vacancies per film were detected.

Increasing the temperature at fixed K_i and increasing K_i at a fixed temperature are often considered equivalent ways

to give the atoms some extra mobility, so that a smoother surface can be grown.¹² Some of the results reported here confirm this picture: the probability to stick to an overhanging site, for example, decreases both raising the temperature and K_i . The steering effect, on the other hand, is only due to the small K_i , and has no equivalent temperature-induced effect.

In this paper we showed that even starting from a flat surface and with a normally incident flux, steering can cause a strong roughening of the surface. The impinging-atom flux becomes inhomogeneous, because surface landing is more frequent near protruding structures. In turn, these structures grow more quickly, creating an instability. When the incoming kinetic energy is very low, even features two atoms high can trigger this effect, increasing the roughness noticeably within the first five monolayers. All the reported results were

obtained at $T \sim 0$ K. At higher temperatures, this roughening will be diminished due to the activation of smoothening diffusion mechanisms. Preliminary results⁷ obtained by simulating the growth process at realistic deposition rates with the TAD method indicate that the steering effect is observable in the roughness of the first few monolayers up to at least $T = 30$ K, which should be accessible to experiment. For thicker films at higher temperatures, statistical fluctuations in surface height may still trigger this instability if the atom-surface interaction range exceeds the effective diffusional smoothening length.

The authors acknowledge fruitful discussions with Bene Poelsema, David Srolovitz, James Sprague, and Tim Germann. This work was supported by the U.S. Department of Energy, Office of Basic Energy Sciences, under DOE Contract No. W-7405-ENG-36.

*Corresponding author; email address: montalenti@t12.lanl.gov

¹S. van Dijken, L. C. Jorritsma, and B. Poelsema, *Phys. Rev. Lett.* **82**, 4038 (1999).

²S. van Dijken, L. C. Jorritsma, and B. Poelsema, *Phys. Rev. B* **61**, 14 047 (2000).

³S. van Dijken, G. Di Santo, and B. Poelsema, *Appl. Phys. Lett.* **77**, 2030 (2000).

⁴W. D. Luedtke and U. Landman, *Phys. Rev. B* **40**, 11 733 (1989).

⁵M. Raible, S. J. Linz, and P. Hänggi, *Phys. Rev. E* **62**, 1691 (2000).

⁶M. R. Sørensen and A. F. Voter, *J. Chem. Phys.* **112**, 9599 (2000).

⁷F. Montalenti, M. R. Sørensen, and A. F. Voter (unpublished).

⁸A. F. Voter, in *Modeling of Optical Thin Films*, edited by

M. R. Jacobson [*Proc. SPIE* **821**, 214 (1987)]; A. F. Voter, Los Alamos Unclassified Technical Report No. LA-UR 93-3901 (1993).

⁹J. W. Evans, *Phys. Rev. B* **43**, 3897 (1991).

¹⁰C. L. Kelchner and A. E. DePristo, *Surf. Sci.* **393**, 72 (1997).

¹¹C. R. Stoldt, K. J. Caspersen, M. C. Bartelt, C. J. Jenks, J. W. Evans, and P. A. Thiel, *Phys. Rev. Lett.* **85**, 800 (2000).

¹²X. W. Zhou, R. A. Johnson, and H. N. G. Wadley, *Acta Metal* **45**, 1513 (1997); C. M. Gilmore and J. A. Sprague, *Phys. Rev. B* **44**, 8950 (1991); R. W. Smith and D. J. Srolovitz, *J. Appl. Phys.* **79**, 1448 (1996).

¹³J. W. Evans, D. E. Sanders, P. A. Thiel, and A. E. DePristo, *Phys. Rev. B* **41**, 5410 (1990).

¹⁴D. E. Sanders, D. M. Halstead, and A. E. DePristo, *J. Vac. Sci. Technol. A* **10**, 1986 (1992).

¹⁵D. E. Sanders and A. E. DePristo, *Surf. Sci.* **254**, 341 (1991).

¹⁶D. M. Halstead and A. E. DePristo, *Surf. Sci.* **286**, 275 (1993).